J. Indian Inst. Sci.
A Multidisciplinary Reviews Journal
ISSN: 0970-4140 Coden-JIISAD

REVIEW ARTICLE

Transporters Through the Looking Glass: An Insight into the Mechanisms of Ion-Coupled Transport and Methods That Help Reveal Them

*Puja Majumder, Aditya Kumar Mallela and Aravind Penmatsa**

Abstract | Cell membranes, despite providing a barrier to protect intracellular constituents, require selective gating for the influx of important metabolites including ions, sugars, amino acids, neurotransmitters and efflux of toxins and metabolic end-products. The machinery involved in carrying out this gating process comprises of integral membrane proteins that use ionic electrochemical gradients or ATP hydrolysis, to drive concentrative uptake or efflux. The mechanism through which ion-coupled transporters function is referred to as alternating-access. In the recent past, discrete modes of alternating-access have been described with the elucidation of new transporter structures and their snapshots in altered conformational states. Despite X-ray structures being the primary sources of mechanistic information, other biophysical methods provide information related to the structural dynamics of these transporters. Methods including EPR and smFRET, have extensively helped validate or clarify ion-coupled transport mechanisms, in a near-native environment. This review seeks to highlight the mechanistic details of ion-coupled transport and delve into the biophysical tools and methods that help in understanding these fascinating molecules.

Keywords: *Secondary active transport, Ion-coupled transport, Alternating-access, Uniport, Symport, Antiport*

1 Introduction

All cells and cellular organelles are protected by one or more hydrophobic membrane bilayers that segregate the internal constituents from the external environment. This phospholipid bilayer serves as a barrier to most compounds that seek to enter or exit the cell. Cells, however, require a controlled exchange of material including ions, metabolites or metabolic end-products and signaling species to maintain normal physiological processes. Consequently, most cellular and organellar membranes have integral membrane proteins in the form of ion-channels and transporters to facilitate this regulated movement of small molecules, vital for the survival of cells.[21,76] While most ion-channels serve as pores for the movement of ions in response to a stimulus, transporters perform the task of gates that move substrates in a controlled fashion into or out of cells.[21]

The direction of substrate movement can be in the direction of the concentration gradient or against it.[81] Transporters that facilitate movement of substrate along the concentration gradient are referred to as uniporters.[81] Transporters that move substrate(s) against their concentration gradients, couple the process to either ATP hydrolysis or to ionic-electrochemical gradients.[74] Primary active transporters use ATP hydrolysis to couple substrate movement, whereas most of the secondary active transporters employ ion-coupling to achieve transport. The direction of ion-flow can occur along the direction of substrate

Molecular Biophysics Unit, Indian Institute of Science, Bangalore 560012, India.
**penmatsa@iisc.ac.in*

Springer IISc Press

movement in case of symporters or against it as observed in antiporters (Fig. 1a).[66]

Ion-coupled transporters in humans are also referred to as solute carriers (SLCs) that form the second largest group of membrane proteins, after GPCRs.[10] Over 450 SLCs are known in humans and a large subset of them are drug targets.[10] Together, SLCs are involved in shuttling ions, sugars, neurotransmitters, amino acids/peptides, lipids, and drugs into or out of cells and organelles.[66] The transporter classification database (TCDB) assigns an enzyme classification style numbering of transport proteins and most of the ion-coupled "porters" are classified under the section 2.A (http://tcdb.org/search/result.php?tc=2.a).[62] Uniporters have very similar structural scaffolds to symporters and antiporters and are generally considered to be secondary active transporters without ion-coupling.[81] Despite their extensive presence and obvious significance in physiology, secondary active transporters/solute carriers remain some of the least-studied among integral membrane protein families, prompting calls for enhanced research on these molecules.[10]

Although quite extensive in their number and substrate-specificity, ion-coupled transporters fall into a small set of structural scaffolds with fewer mechanistic discrepancies.[15] Most secondary active transporters have an inherent symmetry within them and their structural organization reflects this symmetry within the helical repeats (Fig. 1b).[15] The presence of symmetry allows the transporters to undergo alternating-access, the primary mechanism through which substrates are driven across the membrane bilayer.[18, 27] This review focuses on the mechanistic underpinnings of secondary active transport and discusses recent advances in structural and biophysical methods

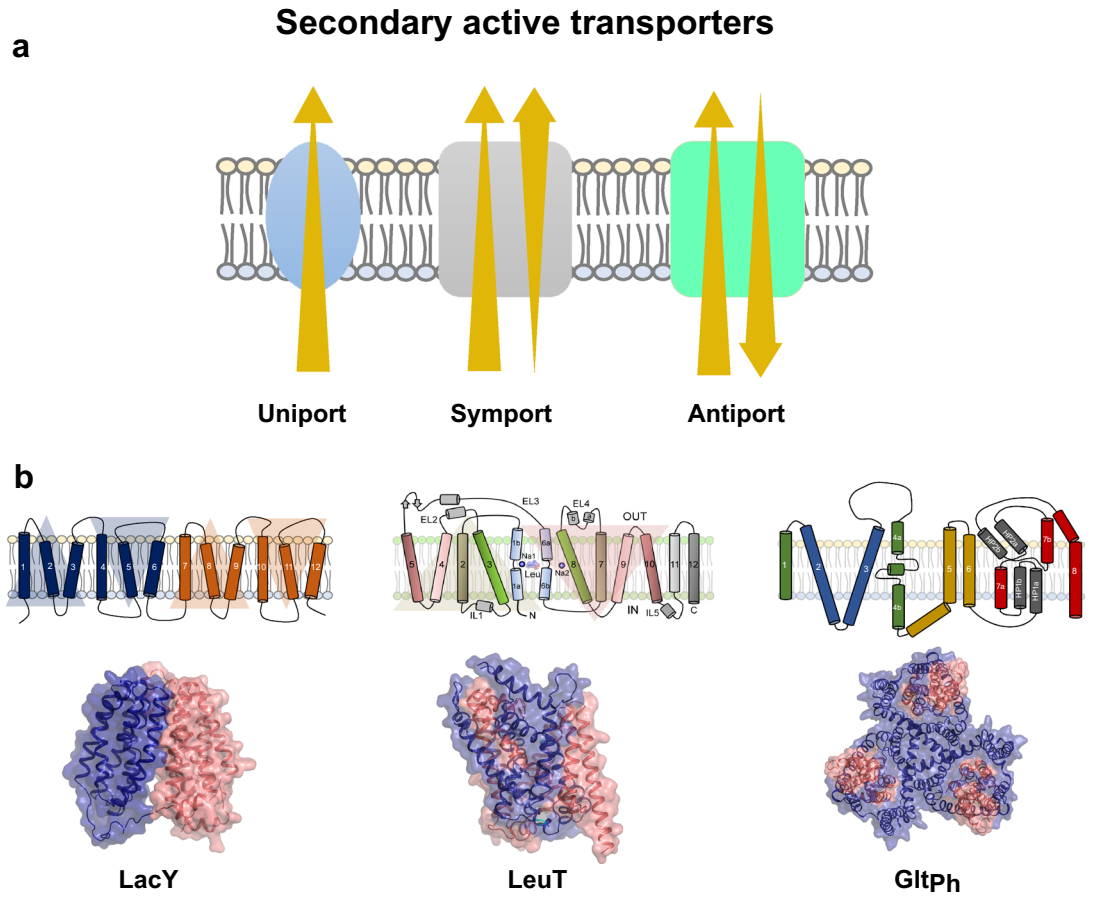

Figure 1: **a** Modes of secondary active transport including uniport (facilitated diffusion), symport and antiport. Direction of ion/substrate flux is indicated by arrows. **b** Membrane topology and X-ray structures of LacY, LeuT and Glt_{Ph}. Topologies represent the broad mechanistic classification of transporters.

that have immensely aided in deciphering the structure, dynamics and functional roles of ion-coupled transporters. Although we primarily focus on transporters as a specific case, the methods described here are generally applicable to all integral membrane proteins.

2 Alternating-Access

The concept of substrate movement across the membrane was envisaged by Peter Mitchell who proposed a carrier hypothesis for substrate translocation in response to a signal, in the form of phosphorylation. The process of translocation was akin to an enzyme catalyzing a biochemical reaction, whereas in case of a transporter, it involves conformational changes to catalyze movement across the membrane.[49]

Jardetzky in 1966 put forth a defined role for carriers wherein he proposed that transporters would undergo conformational changes that alternately expose the binding site to either side of the membrane, but never at the same time.[27] These conformational changes, that occur in response to substrate binding on one side of the compartment followed by its release on the other side, constitutes the alternating-access mechanism (Fig. 2).

In the last two decades, high-resolution structures of transporters across different families have

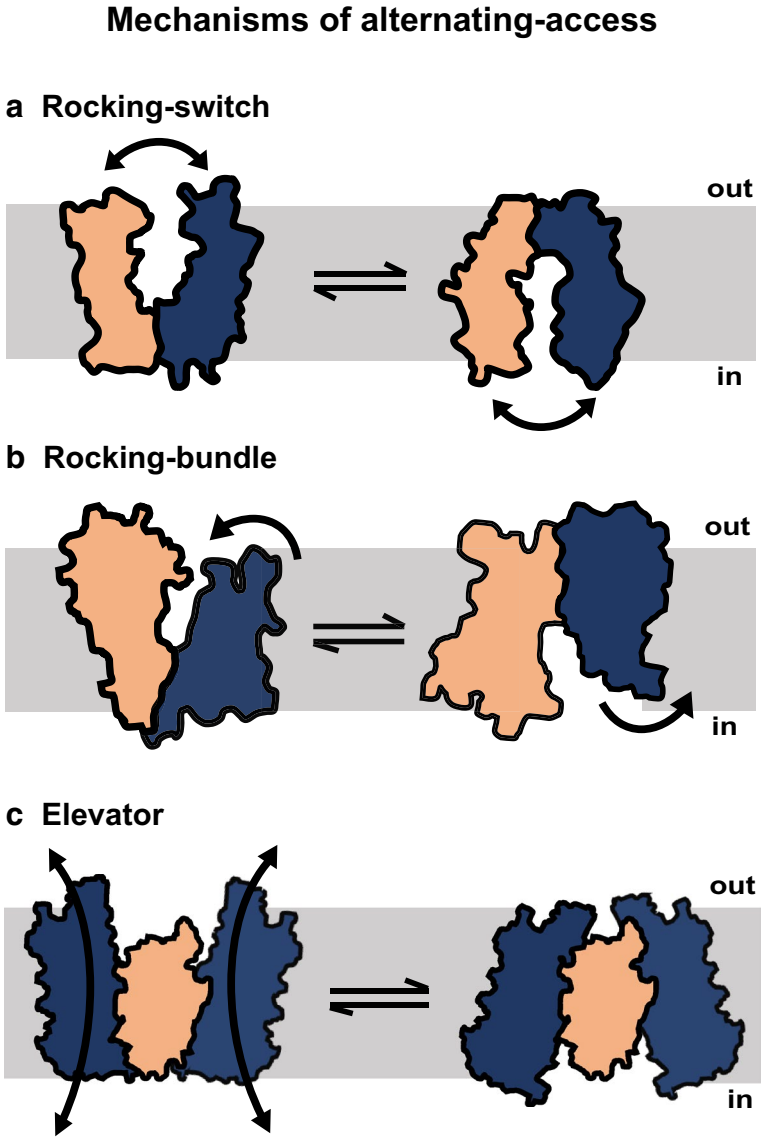

Figure 2: Types of alternating-access mechanisms. Orange and blue colors denote the transporter domains in **a** rocking-switch model, **b** rocking-bundle model. **c** In the elevator model, orange region represents the static oligomerization domain, whereas the blue regions represent the transport domains.

corroborated the presence of symmetrical halves that perform alternating-access, albeit with variations to the primary mechanism. Exceptions to alternating access do occur especially in the chloride channels (CLCs) which transport chloride ions and protons, but given the minimal structural transitions that happen, resemble channel like states.[16] Despite implying the presence of only two states in alternating-access namely, open-to-in (O_{in}) and open-to-out (O_{out}), structures of numerous transporters reveal the presence of asymmetric occluded states including outward-occluded (O_{occ}) or inward-occluded (I_{occ}).[15]

In the recent past, transport was observed to occur in three independent modes while remaining within the bounds of alternating-access. Each mode correlates well with the structural fold of individual molecules (Fig. 2). These are the "rocking-switch" mechanism observed primarily in the major facilitator superfamily (MFS),[34] the multi-drug and toxin extrusion (MATE) family,[59] the SMR (small multidrug resistance)[63] family and the sugars will eventually be exported transporters (SWEETs) (Fig. 2a).[17] Incidentally, the MFS comprises of the largest set of transporters among all secondary active transporters. The second mechanism is the "rocking-bundle" mechanism prevalent in the proteins with the amino acid, polyamine organo-cation superfamily (ApcT) that includes well-studied members like LeuT[67] and Mhp1 (Fig. 2b).[33] A third mechanism common to proteins of the SLC1 family homologues comprising of divalent anion: Na^+ coupled transporters is the "elevator" mechanism (Fig. 2c).[7]

Proton-coupled transport is also observed in the resistance-nodulation-division (RND) family of proteins that comprise of the AcrA/AcrB/TolC complex in Gram −ve bacteria. The ion-coupled transport, in AcrB, is driven by an asymmetric trimer mechanism by coupling proton gradients to antibacterial efflux. The mechanism is akin to the rotor mechanism of the F_1F_0 ATPase system and has been reviewed extensively, elsewhere.[56]

2.1 Rocking-Switch Mechanism

This is the most prevalent mechanism observed across a wide array of the aforementioned families (Table 1; Fig. 2a). The mechanism involves conformational changes occurring upon substrate binding on one side of the membrane, triggering a symmetric rigid body reorientation of helices. This allows the bound substrate to gain access to solvent from the cytosolic compartment and subsequently get released. The SWEET transporters represent a minimal structural organization wherein two three-helix bundles (3 + 3) play a role in the transport process.[71] The SWEET transporter structure revealed a near-symmetric occluded state which is generally not observed in transporters with greater number of helical domains. An interesting case of rocking switch mechanism is the small multidrug resistance family member EmrE, a four TM helix protein that dimerizes to perform drug efflux.[63] To add further credence to this, LacY a prototypical member of the MFS, was observed to retain uptake function despite splitting it into two halves.[5] The ability of these transporters to function as symmetric halves *in trans* indicates the possibility of gene duplication events resulting in formation of the multi-helix transporters as observed in MFS and MATE families.[60]

The MFS and the MATE transporters have six helix bundles that are symmetrically arranged (6 + 6).[81] Each of the six-helix bundle, has two three-helix bundles that are symmetrically related (Fig. 1b). This results in helices 1, 4, 7, 10 being symmetric equivalents and in proximity to the substrate binding site; helices 2, 5, 8, 11 are long and act as rocker helices and partly line the binding site followed by helices 3, 6, 9 and 12 that make the outer ring, acting as support helices and interacting with the membrane environment.[25] In some instances, where two additional helices are observed, as in the case of some peptide–oligopeptide transporters (POTs)[53] and DHA2 members of MFS, the additional helices are positioned in the intracellular loop that links the two six helix bundles forming a 6 + 2+6 arrangement.[60] The structures of a few members of MFS have been determined in different conformational states but no snapshots of a single molecule have been captured in all the states of O_{out}, O_{occ}, I_{occ} or O_{in} (Table 1). We, however, can piece together the transport cycle using snapshots of different molecules in alternate conformational states. For instance, LacY was captured in O_{out} and O_{in} conformations[1, 34] while XylE was observed in O_{occ} and I_{occ} states.[70] Structures of mammalian GluTs, involved in sugar uniport were also captured in O_{out} and O_{in} states.[14, 54] Rocking-switch mode of transport is well observed in case of LacY wherein the two symmetrical halves undergo ~30° movement to alternate from an O_{in} state to O_{out} state.[34]

In the case of mammalian GluTs, in comparison with occluded state structures of XylE, it was observed that the gating occurs through helices bending to create access to the binding site.[54, 70] Hinge movements in helices TM1, TM7 open the extracellular gate and helices TM4, TM10 allow opening of intracellular gate.[54] In most cases, a series of electrostatic interactions are formed and

Table 1: List of transporters with unique structures.

PDB. id	Transporter	Source	Function	Conformations
Mechanism: clamp and switch				
Major facilitator superfamily				
1PV6, 4OAA	LacY	*E. coli*	Lactose: H^+ symport	Inward open, outward open
4GBY, 4JA4, 4JA3	XylE	*E. coli*	Xylose: H^+ symport	Outward open-partly occluded, inward open, partially occluded inward open
3O7P	FucP	*E. coli*	Fucose: H^+ symport	Outward open
1PW4	GlpT	*E. coli*	Glycerol-3-phosphate antiport	Inward open
4APS, 5OXP	PepTst	*S. thermophilus*	Peptide: H^+ symport	Inward open, occluded
4M64	MelB	*Salmonella typhimurium*	Na^+: melibiose symport	Outward open- partially occluded, outward open inactive
4LDS	GlcPse	*S. epidermidis*	Glucose: H^+ symporter	Inward open
4IU8, 4IU9	NarU	*E. coli*	Nitrate: nitrite symport or antiport	Inward open-partially occluded, partially inward open
4JR9, 4U4W	NarK	*E. coli*	Nitrate: nitrite antiport	Inward open, inward open-occluded
5A2N	NRT1.1	*Arabidopsis thaliana*	Nitrate: H^+ symport	Inward open
4J05	PiPT	*Serendipita indica*	Phosphate: H^+ symport	Inward open-occluded
4IKV	GkPOT	*Geobacillus kaustophilus*	Peptide: H^+ symport	Inward open
2XUT	PepTso	*Shewanella oneidensis*	Peptide: H^+ symport	Inward open-partially occluded
4Q65	YbgH	*E. coli*	Peptide: H^+ symport	Inward open
4W6V	YePEPT	*Yersinia enterocolitica*	Peptide: H^+ symport	Inward open
5AYO, 5AYM	BbFPN	*Bdellovibrio bacteriovorus*	Divalent metal ion uniport	Inward open outward open
4zp0	MdfA	*E. coli*	Multidrug: H^+ antiport	Inward open
2GFP	EmrD	*E. coli*	Multidrug: H^+ antiport	Inward open-occluded
3WDO	YajR	*E. coli*		Inward open
4PYP	Glut1	*H. sapiens*	Glucose uniport	Inward open
4ZWC	Glut3	*H. sapiens*	Glucose uniport	Outward open
4YB9, 4YBQ	Glut5	*B. taurus*	Glucose uniport	Inward open
		Rattus norvegicus		Outward open
MATE family transporters				
3MKT	NorM	*Vibrio cholerae*	Multidrug: Na^+/H^+ antiporter	Outward open
4LZ6	DinF	*B. halodurans*	Multidrug: Na^+/H^+ antiporter	Outward open
3VVN	PfMATE	*Pyrococcus furiosus*	Multidrug: Na^+/H^+ antiporter	Outward open
5YCK	CasMATE	*Camelina sativa*	Multidrug: Na^+/H^+ antiporter	Outward open
SWEETs/semiSWEETs				
5CTH	OsSWEET2B	*Oryza sativa*	Na^+: solute symport	Inward open
Mechanism 2: rocking bundle				

Table 1: continued

PDB. id	Transporter	Source	Function	Conformations
LeuT fold proteins (ApcT superfamily)				
2A65	LeuT	*Aquifex aeolicus*	Amino acid: Na^+ symport	Occluded
4US3	MhsT	*Bacillus halodurans*	Na^+: L-tryptophan symport	Inward open-occluded
3GIA	ApcT	*M. jannaschii*	H^+: amino acid symport	Inward open
3DH4	vSGLT	*V. cholerae*	Na^+: sugar symport	
4M48	dDAT	*D. melanogaster*	DA: Na^+/Cl^- symport	Outward open
5I6Z	hSERT	*H. sapiens*	5HT: Na^+/Cl^- symport	Outward open
6C08	SLC38	*D. rerio*	Amino acid: Na^+ symport	Inward open
3HFX	CaiT	*E. coli*	Carnitine: butyrobetaine antiport	Inward open
3WIT	BetP	*C. glutaricum*	Betaine: Na^+ symport	
2JLN, 2JLO	MHP1	*Microbacterium liquefaciens*	Hydantoin: Na^+ symport	Outward open, occluded
3NCY	AdiC	*S. typhimurium*	Arginine/Agmatine antiport	Outward open
Mechanism 3: elevator				
1ZCD	NhaA	*E. coli*	Na^+:H^+ antiport	Inward open
5BZ2	NapA	*Thermus thermophilus*	Na^+:H^+ antiport	Inward open
1XFH	Glt_{Ph}	*Pyrococcus horikoshii*	Dicarboxylate: Na^+ symport	Outward open
5LLM	EAAT1	*H. sapiens*	Glutamate: Na^+ symport	Outward open
5X9R	CitS	*K. pneumoniae*	Citrate: Na^+ symport	Outward open
5E9S	Glt_{TK}	*Thermococcus kodakarensis*	Dicarboxylate: Na^+ symport	
4F35	VcINDY	*Vibrio cholerae*	Divalent anion: Na^+ symport	Inward open
4R0C	YdaH (AbgT family)	*Alcanivorax borkumensis*	Drug efflux	Inward open

broken during the gating process to allow the transport of the substrate. Given the incidence of hinge movements of helices facilitating transport, as compared to large rigid body motions, the MFS transporters resemble a "gated-pore" with the "rocking-switch" mechanism being revised to a "clamp-and-switch" mechanism.[58]

2.2 Rocking-Bundle Mechanism

Members of the amino acid, polyamine, organocation transporters (ApcT) superfamily conform to this transport mechanism.[66] The mechanism is a result of a majority of the TMs, in the transporter, acting as a scaffold and a pair of symmetrical discontinuous helices moving inwards or outwards, to open or close the internal or external gates. While molecules having the rocking-switch mechanism resemble a "V"-shaped architecture, transporters with a rocking-bundle movement have a "K"-shaped architecture (Fig. 2b). This mechanism is best illustrated in case of LeuT, a bacterial amino acid transporter homologous to mammalian neurotransmitter transporters (Table 1).[32, 33] LeuT and eukaryotic neurotransmitter transporters have a pseudo-twofold symmetry between helices 1–5 and 6–10 with two additional helices TM11 and 12 that are outside these symmetric halves (Fig. 1b).[80] While a bulk of the helices along TM3 and TM8 form the scaffold domain, helices 1 and 6 which are discontinuous, form the gating helices. TM1b and TM6a together form the extracellular gate, whereas TM1a and 6b form the cytosolic gates. The discontinuous region of the gating helices, at the core of the transporter, for the substrate and ion-binding sites. LeuT was solved at a high resolution of 1.9 Å with a leucine bound in the binding pocket along with two Na^+ ions that are co-transported with the substrate.[80] The conformation of this state resembled an O_{occ} conformation with

solvent having access to the vestibule, but the binding site is secluded from water due to the F253 residue acting as barrier, preventing solvent access to the binding pocket. Co-crystallization of a bulkier amino acid, tryptophan, allowed the outward movement of TM1b (~9°) and TM6a (5.5°)with a hinge-like movement observed in TM2 (~8°).[68] In the O_{in} state of the transporter TM1a and TM6b move outward to provide access to the substrate binding pocket.[32] TM1a in particular swings out nearly 45° into the membrane environment to facilitate this access.[32] LeuT was never observed in an I_{occ} conformational state, although other homologues like ApcT[65] and MhsT[42] have been observed in this conformation. The gating movements in this family are also associated with the break and formation of salt bridges in the vestibule, much like the rocking-switch mechanism. The movements of the outward gate of LeuT are very similar to movements of dDAT gating helices in its O_{occ} state, suggesting a conservation of this transport mechanism within this superfamily.[78]

2.3 Elevator Mechanism

The elevator mechanism is a specialized form of alternating-access that occurs primarily in oligomeric transporters involved in divalent anion:Na^+ symporters that have structural similarity to *Pyrococcus horikoshii* glutamate transporter Glt_{Ph}.[82] The transporters are oligomeric with the elevator mechanism observed in dimeric and/or trimeric molecules.[15] The molecules can distinctly be separated into the transport domain and oligomerization domains (Fig. 2c). While the oligomerization domain remains fixed in its position, the transport domains translate perpendicular to the membrane plane allowing solvent-access to the substrate binding pocket.[61] The prototypical member of this set of proteins is Glt_{Ph}. Structures with similar transport mechanism have recently been elucidated, including EAAT1,[9] VcINDY,[43], CitS[79] and AbgT (Table 1).[6] Most of these transporters have distinct helical repeats within the oligomerization domain and in the transporter domain.[7] The distinguishing feature for this fold of proteins is the presence of helical hairpin loops HP1 and HP2 that ensconce the substrate binding site and Na^+ binding sites in the vicinity, in close proximity to the discontinuous helix TM7. Glt_{Ph} in its O_{out} state resembles a chalice with a concave vestibule formed by the trimer.[82] Upon substrate binding, the site between HP1 and HP2 loops moves perpendicular to the plane of the membrane by nearly 19 Å and correlated with an 18° twist of the transport domain.[61] The vertical movements were also characterized in VcINDY using mutagenesis and in Glt_{Ph} using smFRET studies. A recent structure of EAAT1 in outward-open state is also likely to follow the same mechanism.[9]

Another group of transporters that have the elevator mechanism but a different structural organization are the Na^+:H^+ antiporters.[38] These dimeric transporters have transporter domains without hairpin loops but have discontinuous helices that are crossed over to form the substrate binding site.[7] The proposition of elevator mechanism, in NHA members, was controversial, although in recent past this mechanism is increasingly accepted.

A large fraction of mechanistic information has come from crystallographic studies of transporters in different conformational states making X-ray crystallography the primary tool for understanding transporter structure and function. However, numerous tools help prepare constructs that are suitable for crystallographic studies and retain transport activity. Additional biophysical methods, useful to study transporter dynamics in solution are included in the later sections of the review.

3 Tools to Aid in Structure Determination of Transporters

3.1 Pre-crystallization Tools

3.1.1 Fluorescence Detection Size Exclusion Chromatography (FSEC)

Gouaux and colleagues pioneered the use of tagging a GFP molecule to membrane proteins and monitoring the crude membrane extract on a size exclusion column linked to a fluorimeter (Fig. 3a).[28] The result was the ability to monitor the profile of the membrane protein without using the purified material. The profile of the GFP-linked membrane protein provides information on the homogeneity, expression level and aggregation propensity in the background of whole cell extract or solubilized membranes in particular detergent. This simple, yet elegant, screening tool has helped immensely in monitoring well-behaved orthologues, optimizing non-ionic detergents, stability measurements and tracking protein behavior upon purification. In recent variations of FSEC, the method was put to use to measure the stability of membrane proteins in different detergent/lipid conditions[24] and also to measure formation of heteromeric

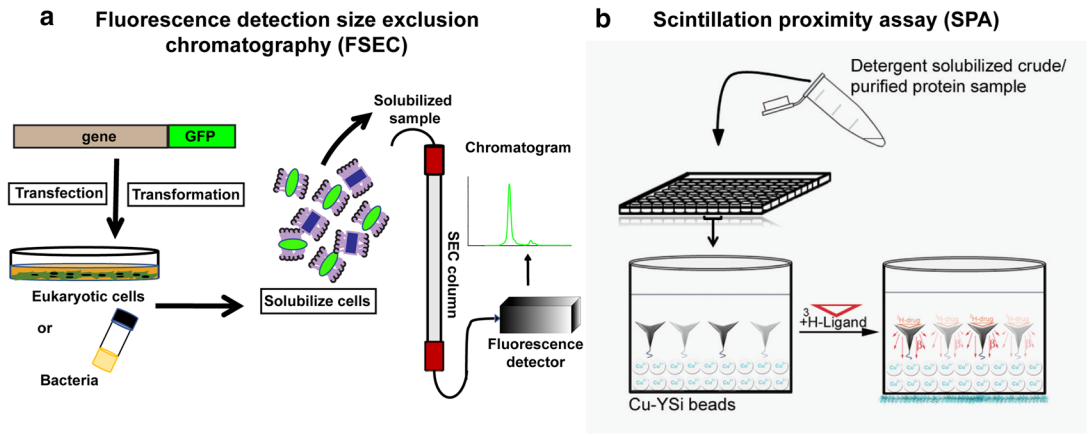

Figure 3: **a** Schematic representation of fluorescence-detection size exclusion chromatography (FSEC) technique using fluorescent protein-tagged membrane proteins, **b** principle of scintillation proximity assay (SPA) done with Cu-YSi scintillant beads and a radiolabeled inhibitor.

complexes.[50] This method is now a standard tool for any lab working on structures of novel transporters or other membrane proteins.

3.1.2 Functional Assays to Monitor Inhibitor Binding

Limitations of FSEC lie in its inability to monitor the function of the transporter. Inhibitor binding can effectively be measured in detergent-solubilized material using radiolabeled drugs/inhibitors. A binding technique that rapidly provides dissociation constants is the scintillation proximity assay (SPA), that employs copper or biotin coated beads that can interact with either a His-tag or a Strep-II tag.[57] A radiolabeled inhibitor that can bind the transporter with high affinity, emits energy on binding the immobilized transporter, leading to scintillation of the beads, resulting in luminescence that can be quantified as binding (Fig. 3b). The method has extensively been applied to transporters including LeuT,[33] dDAT[55] and hSERT.[12] In case of the latter two, it was instrumental in optimizing and isolating thermostable mutants (described below). SPA also works for protein reconstituted in nanodiscs, as observed with LeuT reconstituted into nanodiscs,[52] thereby allowing validation of samples meant for cryoEM data collection. FSEC and SPA are powerful complementary tools to perform pre-crystallization screening.

3.1.3 Construct Engineering Through Mutagenesis

Modification of membrane transporters either through single mutants or large-scale mutagenesis has proven to be an effective strategy towards enhancing the stability and crystallization propensity. This was first reported by James Bowie and colleagues for diacylglycerol kinase (DGK), where twenty out 121 residues in a stretch of sequence, were mutated to cysteines. The experiment yielded two cysteine substitutions with greater thermostability than the native DGK. A combination of the two mutants yielded a significantly thermostabilized molecule.[37] This strategy has since been expanded and employed through alanine or leucine scanning mutagenesis, particularly for the stabilization and structure elucidations of GPCRs[64] and other integral membrane proteins, including transporters.[22] Examples of thermostabilized GPCRs include β1 adrenergic receptors, neurotensin receptor and adenosine receptor.[64,73] The strategy involved creating single alanine mutants through the length of the receptor and identifying mutants that can retain inhibitor binding activity at high temperatures compared to the wild-type constructs. This strategy allowed identification of a small subset of mutants that have a thermostabilizing effect on the receptor and eventually aid in crystallizing them. A similar strategy was employed for the eukaryotic neurotransmitter transporters dDAT and hSERT.[12,55] Briefly, a subset of the entire sequence, primarily in the TM regions were individually mutated to alanine, leucine and phenylalanine resulting in a single mutant library. Individual mutants were then tested for their ability to retain binding towards an inhibitor, either ^{3}H-nisoxetine (dDAT) or ^{3}H-paroxetine (hSERT), when subjected to high temperatures. Mutants that have a consistently improved binding activity

were pooled together, resulting in an additive effect, culminating in thermostabilized constructs. Thermostabilized constructs of dDAT and hSERT retained binding activity at very high temperatures (~60–70 °C). Interestingly, in both studies, thermostabilization led to a complete loss of transport activity resulting in a conformation-locked transporter, stabilized in an outward-open inhibitor-bound state.[12,55]

Besides large-scale scanning mutagenesis, it is quite common to use single or double mutants, towards the purpose of crystallization studies. For instance, LacY, originally determined in the cytosol-open state, carried a single mutation C154G.[1] Subsequently, a periplasmic open state of the transporter was created by a combination of G46W/G262W.[34] Similarly, a multi-drug efflux pump MdfA that belongs to DHA1 of MFS, could be crystallized using a single mutant Q131R.[25] Similarly, in GluT1 a combination of N45T and E329Q led to improved crystals of the transporter.[70] Crystallization of altered conformational states was also made possible by stitching together, mobile domains in transporters. A classic case is the disulfide crosslinking done with Glt_{Ph} to stabilize the O_{in} conformation. Mutations K55C(TM2) in the scaffold domain and A364C(HP2) in the transporter domain allowed the formation of a disulfide cross-link that locked the elevator in Glt_{Ph}, in a cytosol facing conformation.[61]

It is generally observed in projects handling crystallization of recalcitrant molecules, that combinations of mutants, stabilizing certain conformations, coupled with the use of crystallization chaperones, significantly enhance the chances of successful crystallization.[26]

3.1.4 Functional Analysis for Transport Activity

Substrate transport by reconstituted membrane proteins is an evidence for their ability to function independently of other cellular factors. Earlier work involved whole cell-based approaches to study the substrate transport process; conversely, there are some disadvantages as cells have active metabolic mechanisms which can interfere through physical interactions or degradative processes. Transport assays using crude membrane vesicles like spheroplasts or everted vesicles overcome certain drawbacks of doing transport assays in whole cells, while keeping the transporter in its native environment.[20] However, to understand the process of transport with greater clarity and accuracy, we need to see if the transporter can work in isolation. Reconstitution of integral membrane transporters in an artificial membrane, can clarify whether the molecule maintains its functional integrity, in biochemical isolation. Transporters can function as electrogenic or electroneutral, depending on the substrate charge and the number of co-transported ions, during the transport cycle. Based on the characteristic property of transport, different kinds of proteoliposomal transport assays can be devised to monitor activity (Fig. 4).

For instance, the activity of GadC a GABA/glutamate antiporter from *Escherichia coli*, was evaluated using a substrate-trapping approach wherein GABA was trapped inside the reconstituted vesicles and radiolabeled glutamate was added externally to monitor radiolabel accumulation in the vesicle (Fig. 4a).[41] Another approach to monitor H^+-driven antiport is to use the transport of substrate, accompanied with the efflux of protons from the proteoliposome. The changes in internal pH are monitored using a ratiometric pH-sensitive fluorophore, pyranine that is trapped inside the liposomes (Fig. 4b).[13] A recent study employed this method to monitor EmrE's ability to transport guanidinium.[30] In an alternate setup, the Na^+/H^+ antiporter NapA was evaluated through co-reconstitution of F_1F_0 ATP synthase along with NapA. Addition of external ATP generated the required proton gradient for observing NapA transport and the process was monitored using a pH-sensitive dye 9-amino 6-chloro 2-methoxyacridine (ACMA) (Fig. 4c).[38] Recently, measuring ion: substrate stoichiometry was made easier with a method developed by Mindell and colleagues wherein, the transporter reversal potential (E_{rev}) is calculated using known values of $\Delta\psi$ and ion-gradients across the membrane (Table 2; Fig. 4d). The method was applied to measure transport stoichiometry of VcINDY, a bacterial Na^+-coupled succinate transporter and further validated by confirming the known coupling stoichiometry of vSGLT, a bacterial sugar transporter.[51]

3.2 Crystallizations Methods

Michel classified membrane protein crystals into two forms, type I and type II, based on packing of protein molecules in the crystal.[47] While the type I crystals of membrane proteins appear as stacks of bilayers, the type II crystal form resembles lattices formed by soluble proteins, with large aqueous channels surrounded by membrane proteins (Fig. 5a, b). Type I crystals might represent a native bilayer-like arrangement of membrane proteins and are generally desirable over type II

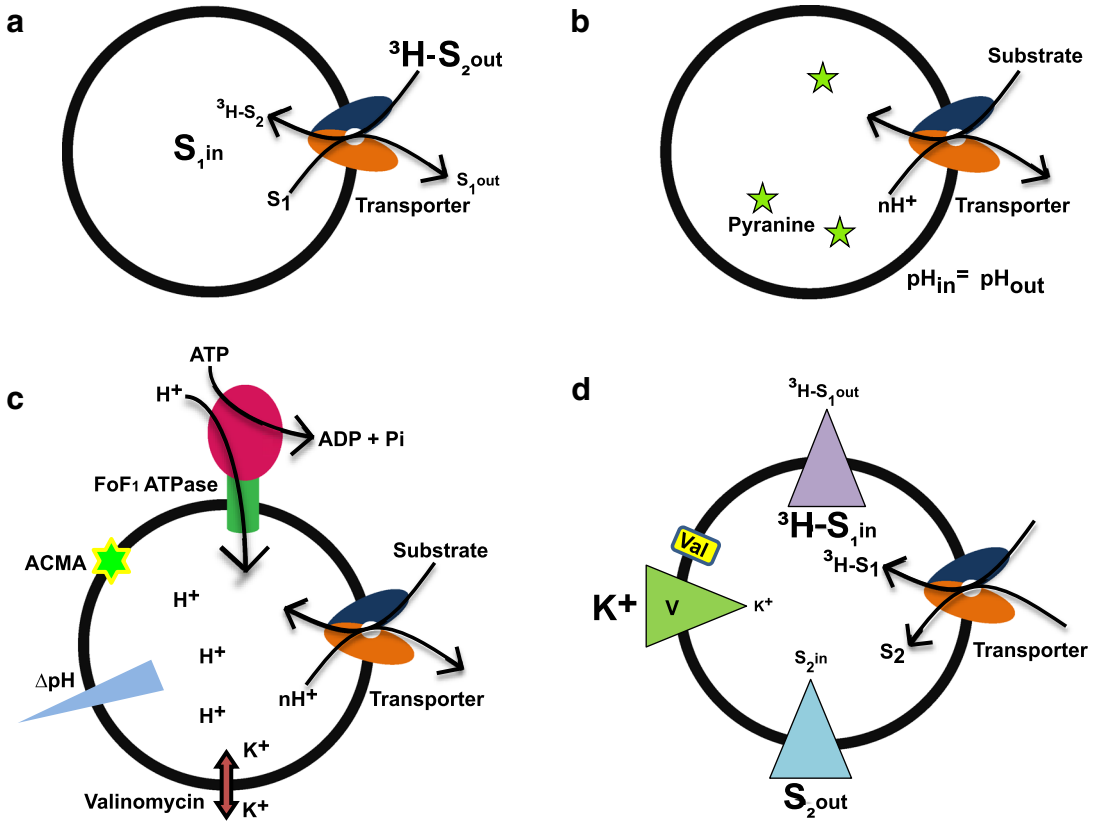

Figure 4: Modes of proteoliposome based transport assays. **a** Substrate trapping method used for an antiporter. The unlabelled substrate (S_1) is trapped inside the liposome and the radiolabeled substrate (^{3}H-S_2) is added externally. The accumulation of radioactive material inside the vesicle is measured. **b** Uniform pH is maintained across the membrane, transport of substrate added from outside causes alteration in pH inside the vesicle and detected using altered pyranine fluorescence. **c** F_1F_0 ATPase co-reconstitution based approach is used for proton-driven antiporters. Addition of ATP in presence of ATPase creates the required pH gradient needed for transport of the substrate. The change in proton concentration due to active transport process is detected by pH sensitive dye ACMA (9-amino 6-chloro 2-methoxyacridine). Valinomycin in presence of potassium ion helps to keep membrane potential constant. **d** Measurement of reversal potential of the membrane at equilibrium is used for electrogenic transporters; radiolabelled substrate (^{3}H-S_1) is trapped in high concentration inside the liposome and unlabelled substrate is added in high concentration outside (S_2). The transport process is initiated by creating different potentials across the membrane using valinomycin in presence of potassium ions. The alteration of radioactive material is measured along with the reversal potential of the membrane.

crystals forms. Lipid-rich crystallization methods including (1) lipidic cubic phase (LCP) (Fig. 5c) and (2) Bicelle-based crystallization (Fig. 5d) have a greater tendency to yield type I crystals of membrane proteins.

Landau and Rosenbusch used lipidic cubic phase to obtain crystals of bacteriorhodopsin by mixing defined ratios of protein solution with a host lipid, monoolein.[36] Monoolein or 9.9 monoacylglycerol (MAG) has a glycerol head group and a single oleic acid with an unsaturation at the 9th carbon. A 3:2 weight ratio mixture of monoolein with water, results in the formation of a clear bicontinuous cubic phase (Pn3m) through self-association.[8] Membrane proteins with or without a crystallization chaperone can be reconstituted into the cubic phase, which upon perturbation by crystallization conditions, results in the formation of lattice contacts leading to crystallization (Fig. 5c). The lattice parameter of the cubic phase and its curvature can be modulated using alternate host lipids with shorter acyl chains or different location of unsaturation which yields cubic phase with reduced curvature and/or altered bilayer thickness. For instance, the bilayer thickness of 7.7 MAG is 41 Å, whereas that of monoolein is 51 Å. The radius of curvature is larger for 7.7 MAG at 56 Å, whereas monoolein

Table 2: Transport equation at E_{rev} for transporters with different substrate:ion stoichiometries.

Process	Transport principle	Stoichiometry
Uniport	$mS^a_{in} \rightarrow mS^a_{out}$	
Symport	$mS^a_{out} + nI^b_{out} \leftrightarrow mS^a_{in} + nI^b_{in}$	$E_{rev} = \Delta\psi = \frac{-60\,mV}{(bn+am)}\left(n \log \frac{[I]_{in}}{[I]_{out}} + m \log \frac{[S]_{in}}{[S]_{out}}\right)$ when $a=-2$, $b=1$ $E_{rev} = \Delta\psi = \frac{-60\,mV}{(n-2m)}\left(n \log \frac{[I]_{in}}{[I]_{out}} + m \log \frac{[S]_{in}}{[S]_{out}}\right)$ when $a=1$, $b=2$ $E_{rev} = \Delta\psi = \frac{-60\,mV}{(2n+m)}\left(n \log \frac{[I]_{in}}{[I]_{out}} + m \log \frac{[S]_{in}}{[S]_{out}}\right)$ when $a=0$, $b=1$ $E_{rev} = \Delta\psi = \frac{-60\,mV}{n}\left(n \log \frac{[I]_{in}}{[I]_{out}} + m \log \frac{[S]_{in}}{[S]_{out}}\right)$
Antiport	$mS^a_{out} + nI^b_{in} \leftrightarrow mS^a_{in} + nI^b_{out}$	$E_{rev} = \Delta\psi = \frac{-60\,mV}{(bn+am)}\left(n \log \frac{[I]_{out}}{[I]_{in}} + m \log \frac{[S]_{in}}{[S]_{out}}\right)$ when $a=-2$, $b=2$ $E_{rev} = \Delta\psi = \frac{-30\,mV}{(n-m)}\left(n \log \frac{[I]_{in}}{[I]_{out}} + m \log \frac{[S]_{in}}{[S]_{out}}\right)$ when $a=1$, $b=2$ $E_{rev} = \Delta\psi = \frac{-60\,mV}{(2n+m)}\left(n \log \frac{[I]_{out}}{[I]_{in}} + m \log \frac{[S]_{in}}{[S]_{out}}\right)$

R is the universal gas constant, ***T*** is the temperature (in °K), ***F*** is the Faraday constant, ***a*** and ***b*** are the substrate and ion charges, respectively, $\Delta\psi$ is the voltage difference across the membrane, ***m*** and ***n*** denotes the number of substrate and ions, respectively. I, S denote ion and substrate, respectively. At equilibrium with conversion to the base 10 log, and approximating ***RT/F*** as 60 mV

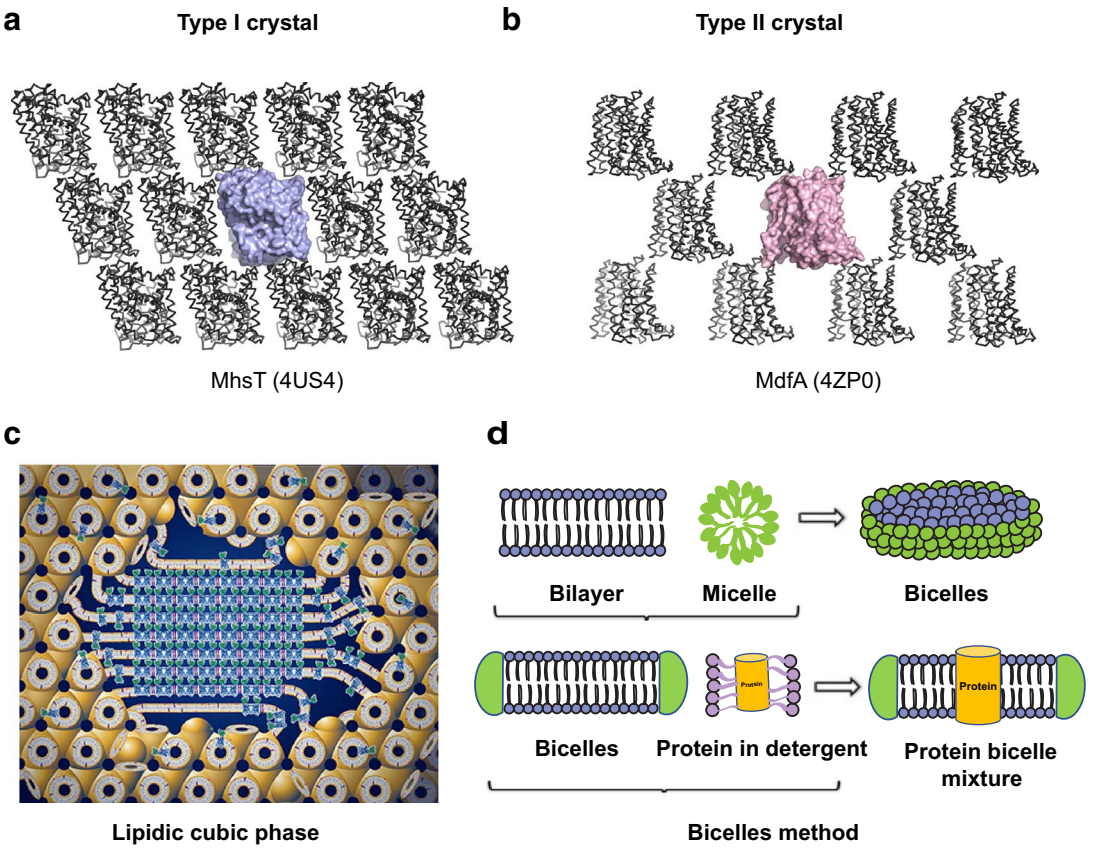

Figure 5: **a** Type I crystal lattice of MhsT (4US4), bacterial sodium driven symporter (NSS family). **b** Type II crystal lattice observed in MdfA (4ZP0), a DHA1 multi-drug efflux transporter. **c** Schematic representation of Pn3m lipidic cubic phase (LCP) shown with induction of crystal nucleation at the centre (figure used from http://cherezov.usc.edu/resources.htm). **d** Pictorial representation of the bicelle crystallisation method.

has 52.2 Å.[48] The use of LCP is quite extensive with GPCRs and is now the predominant method to crystallize them. Transporters also have successful cases where LCP was helpful in obtaining crystals, although detergent based crystallization has also been quite successful in yielding diffraction quality crystals.[19] Crystallization is generally done in glass sandwich plates consuming nanoliter volumes of the cubic phase bolus and reservoir solution. Crystals resulting from LCP tend to have lower solvent content, compared to detergent crystals, resulting in reduced mosaicity. However, the size of the crystals could be small, and prone to radiation damage, requiring data collection and merging of multiple datasets.[40]

Bicelles, on the other hand, are bilayers that have detergent at the periphery to resemble disc-like micelles (Fig. 5d). Bicelles are made by mixing lipids like DMPC and DPPC with detergents like CHAPSO, at ratios around 2.8:1 (lipid:detergent).[72] Bicelles are characterized by their ability to form gel-like state at room temperature and a solution at 4 °C. Membrane proteins incubated with bicelle solution can be used for crystallization screening, similar to detergent micelles. Although a few proteins including LeuT[77] and VDAC were crystallized in bicelles, it remains a minimally used method. Interestingly, both the lipid-rich systems can be doped with other membrane lipids like cholesterol or phospholipids if they are specifically known to improve the behavior of the reconstituted protein.

4 Methods to Evaluate Dynamic Properties of Ion-Coupled Transporters

4.1 EPR/DEER Measurements

Transporters, as observed in the earlier part of the review, tend to undergo small–large-scale domain movements to affect transport. While crystallographic methods are exceptionally powerful in capturing snapshots of transporters in different states, molecular trajectories of how transporters transition from one state to the other, is not very obvious through crystal structures. In the recent past, electron paramagnetic resonance (EPR) measurements using double electron–electron resonance (DEER), has been used extensively to calculate distance distributions using echo between two spin labels located on mobile elements of a transporter[46] (Fig. 6a). DEER measurements are capable of long-range distance measurements up to nearly 6–8 nm which is quite capable of observing the modulation between the scaffold domains and gating elements within secondary active transporters.[46] Measurements are performed by chemical crosslinking of spin labels like 1-oxyl-2,2,5,5-tetramethylpyrroline-3-methyl-methanethiosulfonate (MTSSL), with free cysteines strategically introduced in flexible domains, whose dynamics are to be studied. Site-directed spin labeling (SDSL) also requires the removal of excess free cysteines in the protein of interest, to create cys-less, functional constructs. MTSSL labeled integral membrane protein dynamics can be measured in near-native environments, by studying distance distributions of protein reconstituted into liposomes or nanodiscs.

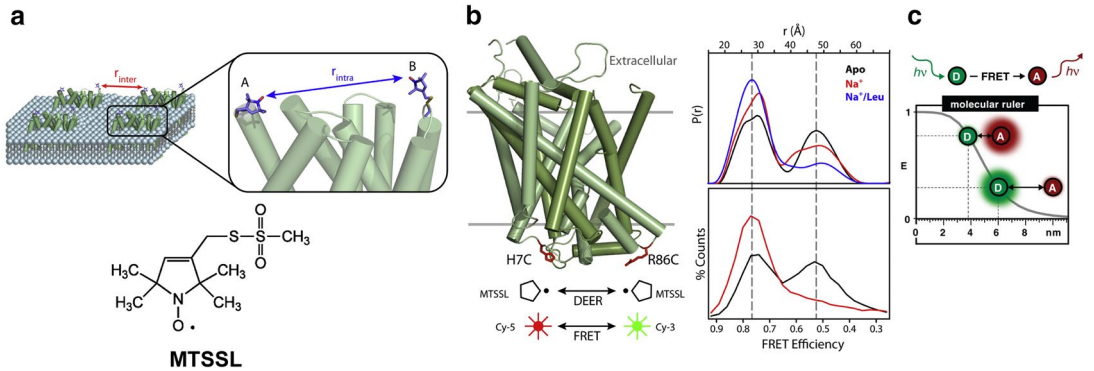

Figure 6: **a** Labeling a transporter at distinct sites using a spin label in case of DEER spectroscopy. **b** Distance distribution calculated from spin echoes in LeuT and their comparison with smFRET studies performed with fluorophores labeled at the same sites (**a**, **b** were adapted from Mchaourab et al.[46] after obtaining the publisher's consent). **c** Estimation of dynamic distance measurement for fluorophores in smFRET experiments. Effective distance lies between 1 and 9 nm (panel adapted from Lerner et al.[39] after publisher's consent).

Measurements performed in LeuT by tagging MTSSL spin labels at extracellular elements in EL2, EL4, TM6b, suggested that the extracellular vestibule has improved solvent access in the presence of Na^+ and in a leucine-free state.[11] Addition of leucine reduces the distance distributions between labels, suggesting the contraction of TM1b, TM6a gates (Fig. 6b). Crystal structure of the substrate-free form of LeuT validated this measurement since it was in an O_{out} state.[32] The high-resolution structure of LeuT in the leucine bound O_{out} state, reveals a clear inward movement of helices and occlusion of the binding pocket thereby correlating with DEER measurements. On the other hand, DEER measurements at the cytosolic elements of LeuT between the N-terminus and TM3 suggested that movement of TM1a is not as prominent as observed in the crystal structure, in solution.[29]

DEER has also been applied to MFS transporters, LacY a symporter and LmrP an antiporter.[44] In LacY, measurements at the cytosolic and the periplasmic regions allowed tracking the substrate-induced rocking switch movements in the transporters.[69] In LmrP, DEER measurements aided in demonstrating pH-dependent gating of the transporter and also demonstrated the role of lipid head groups and their interactions with D68 in motif A, that resulted in modulation of drug efflux in LmrP.[45] In addition to carrying out measurements in detergent-solubilized material, DEER can also be carried out in transporters reconstituted in lipid nanodiscs that allows monitoring the effect of lipids on conformations associated with the transport cycle.[44]

4.2 smFRET Reveals Transporter Dynamics

smFRET is an analogous method to EPR spectroscopy in providing distance information between FRET pairs, specifically labeled on the transporter. The "molecular-ruler" among FRET pairs extends within a dynamic distance range of 1–9 nm allowing monitoring a molecule populating different conformational states (Fig. 6c).[39] Cy-3 and Cy-5 fluorophores were used to label the cytosolic gate of LeuT at H7 (TM1a) and R86 (IL1). SmFRET between the sites, revealed the presence of two distinct states of the molecule that differ in distance of FRET pair by nearly 13 Å, in the absence of Na^+.[84] Incremental addition of Na^+ resulted in the loss of the second state and populated the O_{out} state, giving a glimpse into the gating mechanism. SmFRET studies were carried out on Glt_{Ph} to monitor transport dynamics by labeling the molecule with Cy-3 and Cy-5 to form donor–acceptor pairs. Sites chosen to label were within a distance to exhibit FRET signal but also undergo significant movements during the transport cycle. I294C at the intracellular loop between HP1–TM7 and N378C at the extracellular surface between loop connecting TM7–HP2 were the sites used to label Glt_{Ph}. The smFRET studies revealed that the transport domains can function independent of the other protomers and the apo state can cycle between the O_{out} and O_{in} state rapidly. Upon binding Na^+ and aspartate, the molecule was observed to populate a low FRET O_{out} state while retaining flickers of high FRET state suggesting, quick shifts to the O_{in} conformation.[2] A subsequent study also revealed that the humanized version of the transporter with R276S and M395R mutants results in the unlocking of the transport domains allowing the transporter to sample the inward-open states better, thereby allowing the rapid cycling of the glutamate uptake.[3]

5 Monitoring Interactions of Lipids and Transporters

An underlying theme of studying transporter structure and function is the ability of lipids to interact and modulate transport properties. For instance, it was shown through DEER measurements that phosphatidyl ethanolamine (PE) stabilized the inward-open conformation of LmrP, a multi-drug efflux protein, and cardiolipin was involved in the closure of the extracellular gate in LmrP.[44] In case of BetP, a trimeric betaine transporter with a similar fold as that of LeuT, it was observed to bind POPG lipid in the trimeric interface.[31] The lipids were also observed close to the inner leaflet region surrounding TM1 which forms the cytosolic gate in case of the ApcT family transporters. A similar occurrence of a eukaryotic membrane lipid, cholesterol, was observed bound at the interface created by TM1a, TM5 and TM7 in dDAT suggesting a clear role in its ability to allosterically stabilize an inhibitor bound state of the transporter[55] (Fig. 7a, b). Cholesterol was also observed in the hSERT structure but away from the TM1 site, in the outer leaflet close to the TM12 region.[12] Recent computational studies using coarse grain simulations of hSERT, hDAT, and hNET models have nevertheless, indicated the binding of cholesterol at this site for all three transporters, with varying levels of occupancy.[83]

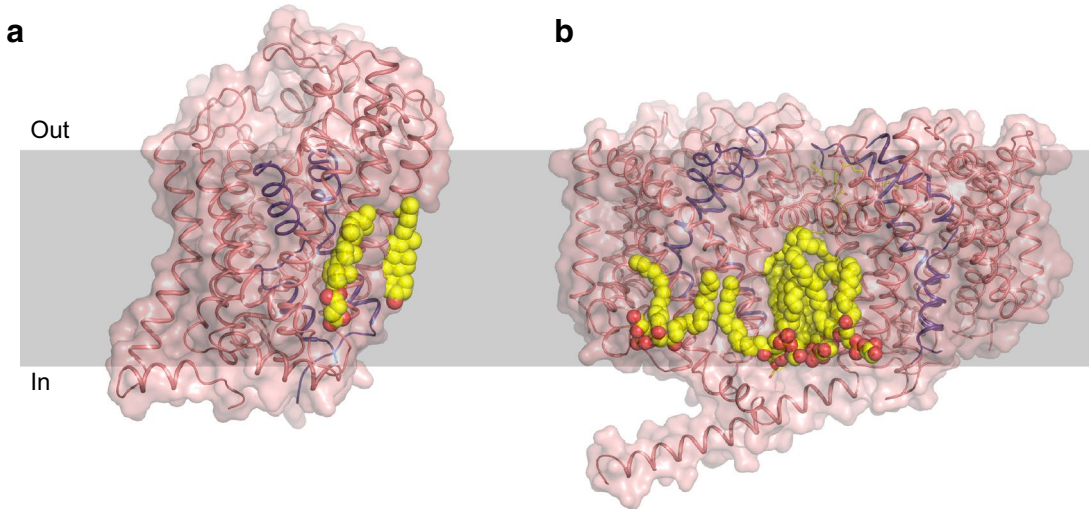

Figure 7: Crystal structures of membrane transporters with bound lipid. **a** dDAT crystal structure (4XP4) bound to cholesterol at the interface of TM1a, 5 and 7 and a cholesteryl hemisuccinate bound at TM2, 7 and 11. **b** POPG molecules found at the interface of the BetP trimer (4C7R). A third molecule in the trimer was removed for clarity. Head group of the lipid is in close proximity to gating helices.

5.1 Mass Spectroscopy of Transporters Associated with Lipid

More often than not, crystal structures do not reveal densities for bound lipid. In the recent past, mass spectroscopy of membrane proteins in gas phase has evolved to obtain signals from intact membrane protein complexes in micelles. This has allowed an unprecedented ability to monitor closely associated lipids that mediate transient or obligate oligomerization in membrane proteins. Carol Robinson and colleagues used ion-mobility mass spectroscopy (IM-MS) to observe that use of non-ionic detergents, above critical micellar concentrations (CMC), allows preservation of the membrane protein complexes, in vacuum using electrospray.[4] At higher acceleration voltages, it was observed that the detergent could dissociate from the oligomer resulting in mass spectra corresponding to membrane protein oligomers.[4] It was observed in a subsequent study that among non-ionic detergents, C8E4 (tetraethylene glycol monooctyl ether) had lower charge states, thereby, facilitating improved characterization of membrane proteins in gas phase.[35] This allowed measurement of the stabilizing effects of protein-bound lipids, on a wide array of integral membrane proteins. A subsequent study from the same group on integral membrane transporters revealed the role of lipids, particularly cardiolipin, in the dimerization of LeuT. It was observed that one molecule of cardiolipin was bound per protomer of LeuT, in the dimer.[23] Cardiolipin was also observed to stabilize sodium: H^+ antiporter NapA dimeric interface with the dimer falling apart, when cardiolipin was completely stripped from the protein.[23]

These advanced methodologies are some of the approaches through which membrane proteins in general and ion-coupled transporters in specific have been characterized in the recent past. With the advent of more crystallographic structures and the application of the aforementioned tools, understanding the broad mechanisms and the subtle variations incorporated by individual transporters in the alternating-access mechanism, will increasingly become evident in the near future.

6 Future Directions and Conclusions

A major tool for studying membrane protein dynamics is through computational studies that are not included in this review, since the focus was on experimental methods. Computational methods, including modeling of alternating access,[18] all atom molecular dynamics and coarse-graining of membrane proteins[83] are extensively being used to tease out information ranging from mechanisms of alternating access, role of water and ions in transport process and lipid interactions of membrane proteins. This information is valuable to bolster the findings from crystallographic studies, since a lot of information on dynamics, binding sites, allostery and transport are not apparent, from molecular coordinates.

In addition to computational tools, the advent of cryoEM to elucidate transporter structures is likely to happen, in the near future. Since most ion-coupled transporters are in the size range of 40–60 kDa, cryoEM is still in a state where high-resolution structural information is difficult to attain. However, novel EM tools like phase plates, and biochemical tools like antibodies that can enhance the size and reduce the conformational heterogeneity, will likely aid in structure determination of transporters through cryoEM in the near future.[75] Given the important roles that the transporters play in physiology and disease and wide array of methodologies available to characterize them, research in ion-coupled transporters is primed for rapid expansion in the near future.

Acknowledgements

The authors would like to thank all members of the Penmatsa Lab for their feedback on the manuscript. PM is supported by the IISc-GATE fellowship. AP is an intermediate fellow of the DBT-Wellcome Trust India Alliance (IA/1/15/2/502063) and a recipient of the Innovative Young Biotechnologist Award (IYBA) (BT/09/IYBA/2015/13) from the Department of Biotechnology (DBT), India.

Received: 19 April 2018 Accepted: 5 June 2018
Published online: 20 June 2018

References

1. Abramson J, Smirnova I, Kasho V, Verner G, Kaback HR, Iwata S (2003) Structure and mechanism of the lactose permease of *Escherichia coli*. Science 301(5633):610–615. https://doi.org/10.1126/science.1088196
2. Akyuz N, Altman RB, Blanchard SC, Boudker O (2013) Transport dynamics in a glutamate transporter homologue. Nature 502(7469):114–118. https://doi.org/10.1038/nature12265
3. Akyuz N, Georgieva ER, Zhou Z, Stolzenberg S, Cuendet MA, Khelashvili G et al (2015) Transport domain unlocking sets the uptake rate of an aspartate transporter. Nature 518(7537):68–73. https://doi.org/10.1038/nature14158
4. Barrera NP, Di Bartolo N, Booth PJ, Robinson CV (2008) Micelles protect membrane complexes from solution to vacuum. Science 321(5886):243–246. https://doi.org/10.1126/science.1159292
5. Bibi E, Kaback HR (1990) In vivo expression of the lacY gene in two segments leads to functional lac permease. Proc Natl Acad Sci USA 87(11):4325–4329
6. Bolla JR, Su CC, Delmar JA, Radhakrishnan A, Kumar N, Chou TH et al (2015) Crystal structure of the *Alcanivorax borkumensis* YdaH transporter reveals an unusual topology. Nat Commun 6:6874. https://doi.org/10.1038/ncomms7874
7. Boudker O, Verdon G (2010) Structural perspectives on secondary active transporters. Trends Pharmacol Sci 31(9):418–426. https://doi.org/10.1016/j.tips.2010.06.004
8. Caffrey M (2009) Crystallizing membrane proteins for structure determination: use of lipidic mesophases. Annu Rev Biophys 38:29–51. https://doi.org/10.1146/annurev.biophys.050708.133655
9. Canul-Tec JC, Assal R, Cirri E, Legrand P, Brier S, Chamot-Rooke J et al (2017) Structure and allosteric inhibition of excitatory amino acid transporter 1. Nature 544(7651):446–451. https://doi.org/10.1038/nature22064
10. Cesar-Razquin A, Snijder B, Frappier-Brinton T, Isserlin R, Gyimesi G, Bai X et al (2015) A call for systematic research on solute carriers. Cell 162(3):478–487. https://doi.org/10.1016/j.cell.2015.07.022
11. Claxton DP, Quick M, Shi L, de Carvalho FD, Weinstein H, Javitch JA et al (2010) Ion/substrate-dependent conformational dynamics of a bacterial homolog of neurotransmitter:sodium symporters. Nat Struct Mol Biol 17(7):822–829. https://doi.org/10.1038/nsmb.1854
12. Coleman JA, Green EM, Gouaux E (2016) X-ray structures and mechanism of the human serotonin transporter. Nature 532(7599):334–339. https://doi.org/10.1038/nature17629
13. Damiano E, Bassilana M, Rigaud JL, Leblanc G (1984) Use of the pH sensitive fluorescence probe pyranine to monitor internal pH changes in *Escherichia coli* membrane vesicles. FEBS Lett 166(1):120–124
14. Deng D, Xu C, Sun P, Wu J, Yan C, Hu M et al (2014) Crystal structure of the human glucose transporter GLUT1. Nature 510(7503):121–125. https://doi.org/10.1038/nature13306
15. Drew D, Boudker O (2016) Shared molecular mechanisms of membrane transporters. Annu Rev Biochem 85:543–572. https://doi.org/10.1146/annurev-biochem-060815-014520
16. Feng L, Campbell EB, Hsiung Y, MacKinnon R (2010) Structure of a eukaryotic CLC transporter defines an intermediate state in the transport cycle. Science 330(6004):635–641. https://doi.org/10.1126/science.1195230
17. Feng L, Frommer WB (2015) Structure and function of SemiSWEET and SWEET sugar transporters. Trends Biochem Sci 40(8):480–486. https://doi.org/10.1016/j.tibs.2015.05.005
18. Forrest LR, Zhang YW, Jacobs MT, Gesmonde J, Xie L, Honig BH et al (2008) Mechanism for alternating access in neurotransmitter transporters. Proc Natl Acad Sci USA 105(30):10338–10343. https://doi.org/10.1073/pnas.0804659105
19. Fowler PW, Orwick-Rydmark M, Radestock S, Solcan N, Dijkman PM, Lyons JA et al (2015) Gating topology of the proton-coupled oligopeptide symporters.

Structure 23(2):290–301. https://doi.org/10.1016/j.str.2014.12.012
20. Futai M (1974) Orientation of membrane vesicles from *Escherichia coli* prepared by different procedures. J Membr Biol 15(1):15–28
21. Gouaux E, Mackinnon R (2005) Principles of selective ion transport in channels and pumps. Science 310(5753):1461–1465. https://doi.org/10.1126/science.1113666
22. Green EM, Coleman JA, Gouaux E (2015) Thermostabilization of the human serotonin transporter in an antidepressant-bound conformation. PLoS ONE 10(12):e0145688. https://doi.org/10.1371/journal.pone.0145688
23. Gupta K, Donlan JAC, Hopper JTS, Uzdavinys P, Landreh M, Struwe WB et al (2017) The role of interfacial lipids in stabilizing membrane protein oligomers. Nature 541(7637):421–424. https://doi.org/10.1038/nature20820
24. Hattori M, Hibbs RE, Gouaux E (2012) A fluorescence-detection size-exclusion chromatography-based thermostability assay for membrane protein precrystallization screening. Structure 20(8):1293–1299. https://doi.org/10.1016/j.str.2012.06.009
25. Heng J, Zhao Y, Liu M, Liu Y, Fan J, Wang X et al (2015) Substrate-bound structure of the *E. coli* multidrug resistance transporter MdfA. Cell Res 25(9):1060–1073. https://doi.org/10.1038/cr.2015.94
26. Hunte C, Michel H (2002) Crystallisation of membrane proteins mediated by antibody fragments. Curr Opin Struct Biol 12(4):503–508
27. Jardetzky O (1966) Simple allosteric model for membrane pumps. Nature 211(5052):969–970
28. Kawate T, Gouaux E (2006) Fluorescence-detection size-exclusion chromatography for precrystallization screening of integral membrane proteins. Structure 14(4):673–681. https://doi.org/10.1016/j.str.2006.01.013
29. Kazmier K, Sharma S, Quick M, Islam SM, Roux B, Weinstein H et al (2014) Conformational dynamics of ligand-dependent alternating access in LeuT. Nat Struct Mol Biol 21(5):472–479. https://doi.org/10.1038/nsmb.2816
30. Kermani AA, Macdonald CB, Gundepudi R, Stockbridge RB (2018) Guanidinium export is the primal function of SMR family transporters. Proc Natl Acad Sci USA 115(12):3060–3065. https://doi.org/10.1073/pnas.1719187115
31. Koshy C, Schweikhard ES, Gartner RM, Perez C, Yildiz O, Ziegler C (2013) Structural evidence for functional lipid interactions in the betaine transporter BetP. EMBO J 32(23):3096–3105. https://doi.org/10.1038/emboj.2013.226
32. Krishnamurthy H, Gouaux E (2012) X-ray structures of LeuT in substrate-free outward-open and apo inward-open states. Nature 481(7382):469–474. https://doi.org/10.1038/nature10737
33. Krishnamurthy H, Piscitelli CL, Gouaux E (2009) Unlocking the molecular secrets of sodium-coupled transporters. Nature 459(7245):347–355. https://doi.org/10.1038/nature08143
34. Kumar H, Kasho V, Smirnova I, Finer-Moore JS, Kaback HR, Stroud RM (2014) Structure of sugar-bound LacY. Proc Natl Acad Sci USA 111(5):1784–1788. https://doi.org/10.1073/pnas.1324141111
35. Laganowsky A, Reading E, Hopper JT, Robinson CV (2013) Mass spectrometry of intact membrane protein complexes. Nat Protoc 8(4):639–651. https://doi.org/10.1038/nprot.2013.024
36. Landau EM, Rosenbusch JP (1996) Lipidic cubic phases: a novel concept for the crystallization of membrane proteins. Proc Natl Acad Sci USA 93(25):14532–14535
37. Lau FW, Nauli S, Zhou Y, Bowie JU (1999) Changing single side-chains can greatly enhance the resistance of a membrane protein to irreversible inactivation. J Mol Biol 290(2):559–564. https://doi.org/10.1006/jmbi.1999.2905
38. Lee C, Yashiro S, Dotson DL, Uzdavinys P, Iwata S, Sansom MS et al (2014) Crystal structure of the sodium–proton antiporter NhaA dimer and new mechanistic insights. J Gen Physiol 144(6):529–544. https://doi.org/10.1085/jgp.201411219
39. Lerner E, Cordes T, Ingargiola A, Alhadid Y, Chung S, Michalet X et al (2018) Toward dynamic structural biology: two decades of single-molecule Forster resonance energy transfer. Science 359(6373):eaan1133. https://doi.org/10.1126/science.aan1133
40. Liu W, Wacker D, Wang C, Abola E, Cherezov V (2014) Femtosecond crystallography of membrane proteins in the lipidic cubic phase. Philos Trans R Soc Lond B Biol Sci 369(1647):20130314. https://doi.org/10.1098/rstb.2013.0314
41. Ma D, Lu P, Shi Y (2013) Substrate selectivity of the acid-activated glutamate/gamma-aminobutyric acid (GABA) antiporter GadC from *Escherichia coli*. J Biol Chem 288(21):15148–15153. https://doi.org/10.1074/jbc.M113.474502
42. Malinauskaite L, Quick M, Reinhard L, Lyons JA, Yano H, Javitch JA et al (2014) A mechanism for intracellular release of Na^+ by neurotransmitter/sodium symporters. Nat Struct Mol Biol 21(11):1006–1012. https://doi.org/10.1038/nsmb.2894
43. Mancusso R, Gregorio GG, Liu Q, Wang DN (2012) Structure and mechanism of a bacterial sodium-dependent dicarboxylate transporter. Nature 491(7425):622–626. https://doi.org/10.1038/nature11542
44. Martens C, Stein RA, Masureel M, Roth A, Mishra S, Dawaliby R et al (2016) Lipids modulate the conformational dynamics of a secondary multidrug transporter. Nat Struct Mol Biol 23(8):744–751. https://doi.org/10.1038/nsmb.3262
45. Masureel M, Martens C, Stein RA, Mishra S, Ruysschaert JM, McHaourab HS et al (2014) Protonation drives the conformational switch in the multidrug transporter LmrP. Nat Chem Biol 10(2):149–155. https://doi.org/10.1038/nchembio.1408

46. McHaourab HS, Steed PR, Kazmier K (2011) Toward the fourth dimension of membrane protein structure: insight into dynamics from spin-labeling EPR spectroscopy. Structure 19(11):1549–1561. https://doi.org/10.1016/j.str.2011.10.009
47. Michel H (1983) Crystallization of membrane proteins. [Review]. Trends Biochem Sci 8(2):5
48. Misquitta LV, Misquitta Y, Cherezov V, Slattery O, Mohan JM, Hart D et al (2004) Membrane protein crystallization in lipidic mesophases with tailored bilayers. Structure 12(12):2113–2124. https://doi.org/10.1016/j.str.2004.09.020
49. Mitchell P (1957) A general theory of membrane transport from studies of bacteria. Nature 180(4577):134–136
50. Morales-Perez CL, Noviello CM, Hibbs RE (2016) Manipulation of subunit stoichiometry in heteromeric membrane proteins. Structure 24(5):797–805. https://doi.org/10.1016/j.str.2016.03.004
51. Mulligan C, Fenollar-Ferrer C, Fitzgerald GA, Vergara-Jaque A, Kaufmann D, Li Y et al (2016) The bacterial dicarboxylate transporter VcINDY uses a two-domain elevator-type mechanism. Nat Struct Mol Biol 23(3):256–263. https://doi.org/10.1038/nsmb.3166
52. Nasr ML, Singh SK (2014) Radioligand binding to nanodisc-reconstituted membrane transporters assessed by the scintillation proximity assay. Biochemistry 53(1):4–6. https://doi.org/10.1021/bi401412e
53. Newstead S, Drew D, Cameron AD, Postis VL, Xia X, Fowler PW et al (2011) Crystal structure of a prokaryotic homologue of the mammalian oligopeptide-proton symporters, PepT1 and PepT2. EMBO J 30(2):417–426. https://doi.org/10.1038/emboj.2010.309
54. Nomura N, Verdon G, Kang HJ, Shimamura T, Nomura Y, Sonoda Y et al (2015) Structure and mechanism of the mammalian fructose transporter GLUT5. Nature 526(7573):397–401. https://doi.org/10.1038/nature14909
55. Penmatsa A, Wang KH, Gouaux E (2013) X-ray structure of dopamine transporter elucidates antidepressant mechanism. Nature 503(7474):85–90. https://doi.org/10.1038/nature12533
56. Pos KM (2009) Drug transport mechanism of the AcrB efflux pump. Biochim Biophys Acta 1794(5):782–793. https://doi.org/10.1016/j.bbapap.2008.12.015
57. Quick M, Javitch JA (2007) Monitoring the function of membrane transport proteins in detergent-solubilized form. Proc Natl Acad Sci USA 104(9):3603–3608. https://doi.org/10.1073/pnas.0609573104
58. Quistgaard EM, Low C, Guettou F, Nordlund P (2016) Understanding transport by the major facilitator superfamily (MFS): structures pave the way. Nat Rev Mol Cell Biol 17(2):123–132. https://doi.org/10.1038/nrm.2015.25
59. Radchenko M, Symersky J, Nie R, Lu M (2015) Structural basis for the blockade of MATE multidrug efflux pumps. Nat Commun 6:7995. https://doi.org/10.1038/ncomms8995
60. Reddy VS, Shlykov MA, Castillo R, Sun EI, Saier MH Jr (2012) The major facilitator superfamily (MFS) revisited. FEBS J 279(11):2022–2035. https://doi.org/10.1111/j.1742-4658.2012.08588.x
61. Reyes N, Ginter C, Boudker O (2009) Transport mechanism of a bacterial homologue of glutamate transporters. Nature 462(7275):880–885. https://doi.org/10.1038/nature08616
62. Saier MH Jr, Tran CV, Barabote RD (2006) TCDB: the transporter classification database for membrane transport protein analyses and information. Nucleic Acids Res 34(Database issue):D181–D186. https://doi.org/10.1093/nar/gkj001
63. Schuldiner S (2009) EmrE, a model for studying evolution and mechanism of ion-coupled transporters. Biochim Biophys Acta 1794(5):748–762. https://doi.org/10.1016/j.bbapap.2008.12.018
64. Serrano-Vega MJ, Magnani F, Shibata Y, Tate CG (2008) Conformational thermostabilization of the beta1-adrenergic receptor in a detergent-resistant form. Proc Natl Acad Sci USA 105(3):877–882. https://doi.org/10.1073/pnas.0711253105
65. Shaffer PL, Goehring A, Shankaranarayanan A, Gouaux E (2009) Structure and mechanism of a Na^+-independent amino acid transporter. Science 325(5943):1010–1014. https://doi.org/10.1126/science.1176088
66. Shi Y (2013) Common folds and transport mechanisms of secondary active transporters. Annu Rev Biophys 42:51–72. https://doi.org/10.1146/annurev-biophys-083012-130429
67. Singh SK (2008) LeuT: a prokaryotic stepping stone on the way to a eukaryotic neurotransmitter transporter structure. Channels (Austin) 2(5):380–389
68. Singh SK, Piscitelli CL, Yamashita A, Gouaux E (2008) A competitive inhibitor traps LeuT in an open-to-out conformation. Science 322(5908):1655–1661. https://doi.org/10.1126/science.1166777
69. Smirnova I, Kasho V, Choe JY, Altenbach C, Hubbell WL, Kaback HR (2007) Sugar binding induces an outward facing conformation of LacY. Proc Natl Acad Sci USA 104(42):16504–16509. https://doi.org/10.1073/pnas.0708258104
70. Sun L, Zeng X, Yan C, Sun X, Gong X, Rao Y et al (2012) Crystal structure of a bacterial homologue of glucose transporters GLUT1-4. Nature 490(7420):361–366. https://doi.org/10.1038/nature11524
71. Tao Y, Cheung LS, Li S, Eom JS, Chen LQ, Xu Y et al (2015) Structure of a eukaryotic SWEET transporter in a homotrimeric complex. Nature 527(7577):259–263. https://doi.org/10.1038/nature15391
72. Ujwal R, Abramson J (2012) High-throughput crystallization of membrane proteins using the lipidic bicelle method. J Vis Exp 59:e3383. https://doi.org/10.3791/3383
73. Vaidehi N, Grisshammer R, Tate CG (2016) How can mutations thermostabilize G-protein-coupled

receptors? Trends Pharmacol Sci 37(1):37–46. https://doi.org/10.1016/j.tips.2015.09.005
74. Vinothkumar KR, Henderson R (2010) Structures of membrane proteins. Q Rev Biophys 43(1):65–158. https://doi.org/10.1017/S0033583510000041
75. Vinothkumar KR, Henderson R (2016) Single particle electron cryomicroscopy: trends, issues and future perspective. Q Rev Biophys 49:e13. https://doi.org/10.1017/S0033583516000068
76. von Heijne G (2006) Membrane-protein topology. Nat Rev Mol Cell Biol 7(12):909–918. https://doi.org/10.1038/nrm2063
77. Wang H, Elferich J, Gouaux E (2012) Structures of LeuT in bicelles define conformation and substrate binding in a membrane-like context. Nat Struct Mol Biol 19(2):212–219. https://doi.org/10.1038/nsmb.2215
78. Wang KH, Penmatsa A, Gouaux E (2015) Neurotransmitter and psychostimulant recognition by the dopamine transporter. Nature 521(7552):322–327. https://doi.org/10.1038/nature14431
79. Wohlert D, Grotzinger MJ, Kuhlbrandt W, Yildiz O (2015) Mechanism of Na(+)-dependent citrate transport from the structure of an asymmetrical CitS dimer. eLife 4:e09375. https://doi.org/10.7554/eLife.09375
80. Yamashita A, Singh SK, Kawate T, Jin Y, Gouaux E (2005) Crystal structure of a bacterial homologue of Na^+/Cl^- dependent neurotransmitter transporters. Nature 437(7056):215–223. https://doi.org/10.1038/nature03978
81. Yan N (2015) Structural biology of the major facilitator superfamily transporters. Annu Rev Biophys 44:257–283. https://doi.org/10.1146/annurev-biophys-060414-033901
82. Yernool D, Boudker O, Jin Y, Gouaux E (2004) Structure of a glutamate transporter homologue from *Pyrococcus horikoshii*. Nature 431(7010):811–818. https://doi.org/10.1038/nature03018
83. Zeppelin T, Ladefoged LK, Sinning S, Periole X, Schiott B (2018) A direct interaction of cholesterol with the dopamine transporter prevents its out-to-inward transition. PLoS Comput Biol 14(1):e1005907. https://doi.org/10.1371/journal.pcbi.1005907
84. Zhao Y, Terry D, Shi L, Weinstein H, Blanchard SC, Javitch JA (2010) Single-molecule dynamics of gating in a neurotransmitter transporter homologue. Nature 465(7295):188–193. https://doi.org/10.1038/nature09057

Puja Majumder has a bachelor's degree from St. Xavier's college, Kolkata in Microbiology and a Master's degree in Biotechnology from Jawaharlal Nehru University, Delhi. She joined the Indian Institute of Science as a Ph.D. student in 2015, in the Molecular Biophysics Unit. As a graduate student in the Penmatsa Lab, her research is focused on the structural and biophysical characterization of ion-coupled transporters.

Aditya Kumar Mallela is a project student at the Molecular Biophysics Unit, India institute of Science. He obtained his master's degree in pharmacology from Nirma University, Ahmedabad. He is currently working on the biophysical characterization and structure elucidation of proton-coupled antiporters.

Aravind Penmatsa is an assistant professor at the Molecular Biophysics Unit, Indian Institute of Science. He has a Ph.D. from the Centre for Cellular and Molecular Biology, Hyderabad, where his research focused on the structural and biophysical properties of calcium-binding proteins. His postdoctoral fellowship at the Vollum Institute, Oregon Health and Science University, focused on the structure elucidation of the dopamine transporter. At IISc, the Penmatsa Laboratory studies the structural, mechanistic and pharmacological aspects of transporters involved in neurotransmitter transport and antibacterial efflux.